Archives of Materials Science and Engineering

Volume 74
Issue 1
July 2015
Pages 5-14

International Scientific Journal
published monthly by the
World Academy of Materials
and Manufacturing Engineering

Initial results on the development of niobium plasma carburizing

S.F. Brunatto [a,*], K.S. Velez [b]

[a] Department of Mechanical Engineering, Plasma Assisted Manufacturing Technology & Powder Metallurgy Group, Federal University of Paraná (UFPR), 81531-980, Curitiba, PR, Brazil
[b] Materials Science and Engineering Post-Graduation Program (PIPE), Plasma Assisted Manufacturing Technology & Powder Metallurgy Group, Federal University of Paraná (UFPR), 81531-980, Curitiba, PR, Brazil
* Corresponding e-mail address: brunatto@ufpr.br

ABSTRACT

Purpose: The aim of this work is to present the main initial results on the development of the niobium plasma carburizing process.

Design/methodology/approach: The development of a new pulsed direct current power supply plasma assisted thermo-chemical treatment process for niobium.

Findings: Niobium plasma carburizing can be successfully carried out, and niobium carbide phases can be obtained in the treated surface.

Research limitations/implications: The risk of arc formation during the surface treatment can be overcome by optimizing the discharge geometry.

Practical implications: The highly reactive plasma atmosphere is an advantage regarding the other conventional treatment processes.

Originality/value: It is a new process development, and in this moment it is being considered to be patented in Brazil by the authors.

Keywords: Niobium; Plasma carburizing; Instrumented nanoindentation

Reference to this paper should be given in the following way:

S.F. Brunatto, K.S. Velez, Initial results on the development of niobium plasma carburizing, Archives of Materials Science and Engineering 74/1 (2015) 5-14.

MATERIALS

1. Introduction

DC plasma assisted carburizing is easily obtained by applying a potential difference between electrodes placed in a gas medium under low pressure, typically formed by an Ar + H_2 + CH_4 containing gas mixture. In this case, free electrons and positive ions present in the gas mixture are accelerated by the electric field, and collisions with neutral gas species occur, leading the gas to be ionized. The gas ionization originates a bright-aspect discharge which characterizes the formation of plasma [1-6], resulting in a classical example of cold plasma application. In DC materials processing, plasma carburizing [6-9] is very similar to the very well established plasma assisted nitriding [10,11], and sintering [12,13], processes. Argon (neutral gas) is used for the purpose of sample heating. Hydrogen (important reducing gas) plays important role on the interaction with niobium oxide layer present in the part surface.

From the different possible regimes of discharge that can be established according to current-voltage characteristic of a DC plasma system [3,4], the abnormal glow regime presents special interest for carburizing purpose. This is due to the fact that the cathode (also comprising the parts to be treated) is completely covered by the glow discharge, which is an essential condition to perform a homogeneous treatment in the referred process. In addition, in this discharge regime, the electrical current is proportional to the applied voltage. This allows the application of high voltages resulting in increased ionization of the gas, thus in an appropriate current and cathode temperature control.

One significant aspect to be considered in DC plasma assisted carburizing is in the heating mode by which the carburizing temperature is achieved and the energy is transferred to the parts in treatment [12,15]. For parts acting as cathode, heating to the carburizing temperature is a direct consequence of the part surface plasma species bombardment, for which sputtering is also present [16]. For the cathode heating mode, no hot wall system (system chamber wall presenting electrical resistance) is necessary.

Figure 1 shows an *in situ* view of a linear glow discharge working in abnormal regime, during a niobium plasma carburizing treatment, in the cathode heating mode. In this case, a glow discharge presenting intense bright aspect is formed between the cathode and the anode, and it completely surrounds the sample in treatment, if sufficient energy is supplied by an external source. The intense bright of the glow is related to the temperature necessary to perform the carburizing treatment, being due to the power transferred to the plasma, by usually using a DC square waveform pulsed power supply. In this case, the substrate (cathode) heating due to the energy transfer provided by the plasma species bombarding the cathode is a consequence of the kinetics energy converted in heat by momentum transfer.

Regarding the processing parameters, temperature is far the most important, since plasma carburizing is also a thermally activated process. In the same way, the role of the gas mixture composition is worth to be stressed. Gas mixture composition, usually comprised by $Ar + H_2 + CH_4$, as previously presented, is directly related with the reactivity of the plasma as by the species availability as by the energy of the plasma species. In this case, the gas ionization/excitation/dissociation rates can be easily modified, thus directly impacting on the plasma reactivity and density. It is to be remembered that atomic carbon, besides being the reactive component in gas phase responsible to lead the sample to the carburized state, it also plays important role in plasma carburizing process as a strong

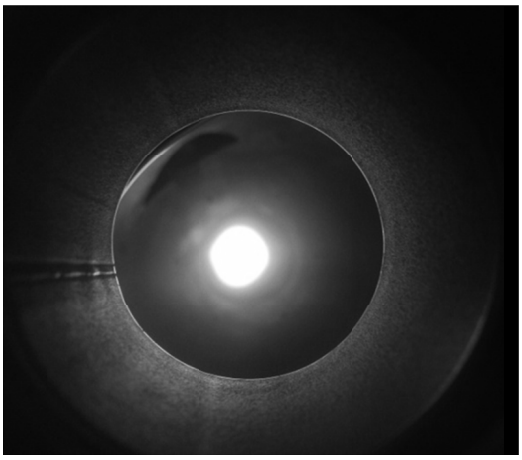

Fig. 1. *In situ* view of an abnormal regime glow discharge, during niobium plasma carburizing treatment, in cathode heating mode

reducing component, directly acting on the reduction of the stable niobium oxide layer present on niobium substrate surface during plasma processing.

Otherwise, as presented in [17], nitrides and carbides of transition metals of groups IV, V and VI usually show physical-chemical characteristics of interest in mechanical field as high hardness, good abrasion wear resistance, corrosion resistance and excellent thermal stability [18-20]. Due to it, these materials are good candidates to have their surfaces altered by thermochemical treatments [21-26]. Too little or nothing has been met on plasma carburizing of niobium in specialized literature. Niobium is a refractory and ductile b.c.c. (body centered cubic) metal [27]. According to [28], high purity annealed niobium presents hardness of 80 HV, tensile strength of 275 MPa, yield strength of 207 MPa, elastic modulus of 103 GPa, and virtually unlimited elongation expressed in percent values. In its pure state, at high temperatures in the presence of oxygen, it promptly oxidizes but, when bonded with carbon, it forms high stable carbides. Regarding niobium carbides, they apparently are chemically inert to most of the applications. So, similar to that verified for niobium nitrides, which have been increasingly studied and developed for different applications (use in high temperature, microelectronics, micromechanics, superconductivity, and others [29,30-34]), one also should expect the same for niobium carbides.

In this work, it is shown one possible way to obtain niobium carbide, presenting the first results on the plasma carburizing process development of niobium substrates. Emphasis is also given on the main challenges related to the risk of arc formation and temperature control during the

surface treatment process, allied to aspects of the carburized layer formation kinetics and the phases formed in the niobium treated surfaces.

2. Experimental procedures

Niobium samples were cut by wire electrical discharge machining (WEDM) in dimensions of 10 x 10 x 4 mm^3 from 98.9% purity and 90% reduction cold-rolled niobium bar from CBMM - *Companhia Brasileira de Metalurgia e Mineração*. Annealing treatment of the cold-worked niobium samples was carried out in vacuum furnace at 1.33 Pa (10^{-2} Torr) pressure, in the temperature of 1000°C, for a time of 60 min. The samples were ground using 220, 320, 400, 600 and 1200 SiC sand-paper. Aiming to obtain the finishing of the testing surfaces, samples were initially polished using 1.0 μm diamond paste, and finally polished with 0.05 μm Al_2O_3 solution.

Plasma carburizing was performed at 1100°C, for treatment times of 10, 90, and 200 minutes, using a gas mixture 0.99 (80% Ar + 20% H_2) + 0.01 CH_4, under a flow of 300 sccm, pressure of 1200 Pa (9 Torr). Treatments were carried out using 4.16 kHz square-wave pulsed DC power supply, using an average peak voltage of 680 V, and a pulse period of 240 μs. The heating of the sample to the treatment temperature was achieved by plasma species bombardment only. The sample temperature was controlled by varying the duty cycle (or the switched-on time of the pulse, *ton*), and it was measured by means of a chromel-alumel thermocouple (type K, and 1.5 mm diameter), which was inserted to a depth of 8 mm inside the sample. The sample holder was machined from a steel bar presenting composition similar to the AISI 1008 steel. Before the carburizing stage, sample was cleaned using H_2 glow discharge at 300°C, for 15 min, and pressure of 400 Pa (3 Torr). After this step, the gas pressure was adjusted to the specified value of 1200 Pa (9 Torr), and the sample was heated up to the carburizing temperature at a heating rate on the order of 0.45°Cs^{-1}.

The 10 x 10 mm^2 sample surfaces were characterized by SEM, XRD, nanoindentation, and high precision 3D profile analysis laser interferometry techniques. The 2D profiles measured at the studied surfaces were performed in accordance with ISO 25178, using a Talysurf CCI - Lite Non-contact 3D Profiler, from Taylor Hobson. In this case, measurements were performed for all the studied surfaces, using a area of 1.5 x 1.5 mm^2, with a resolution of 1632 μm, 1633 μm, and 0.01 nm, for X, Y, and Z axis, respectively. The 3D to 2D roughness parameters conversion was carried out using the diagonal line of the measured 1.5 x 1.5 mm^2 square area, in accordance with the ISO 4287 standard.

Nanoindenter XP-MTS System was used to determine the hardness and to perform scratch testing of the studied surfaces. The hardness versus penetration depth curves were obtained on the average of 25 (5 x 5 matrix) indentations with 100 μm spacing, using a Berkovich type indenter, and 12 charge-discharge cycles, for loads up to 400 mN (40 gf) and 10 s loading time. The scratch tests were performed using loadings from 0 to 400 mN (0 to 40 gf), scratch length of 600 μm and indenter translation velocity of 10 μms^{-1}. Topography profiles of the studied surfaces were also obtained, by making the indenter tip to run along about 700 μm length. In this case, penetration profiles for the scratches during loading and after unloading were also determined aiming to characterize the penetration residual morphology, and thus to confront the elastic and plastic behavior of the carburized surfaces in relation to those of the untreated niobium.

The identification of the phases formed at the studied surfaces was carried out by the X-Ray Diffraction (XRD) technique, using a Shimadzu XRD 7000 X-ray diffractometer, with CuKα radiation, at Bragg-Brentano configuration, for 2θ angles ranging from 10 to 120º, and scanning speed of 1ºs^{-1}. On the other hand, Scanning Electron Microscopy (SEM) analysis was performed aiming to determine the surface morphology of the studied samples and the characteristics of the cavitation eroded surfaces, using TESCAN-VEGA3-LMU equipment.

3. Results and discussion

3.1. Challenges on the development of the niobium plasma carburizing process

In Fig. 2 it is shown, in brief, the main results achieved on the development of the carburizing process of niobium samples. It indicates the evolution of the temperature (*T*), switched-on time of the pulse (*ton*) or duty cycle, and current (*I*) as a function of the treatment time (thermal cycle) for the niobium samples carburized at 200 min. The experiments comprised the use of different cathode assemblages, using distinct types of sample holders and materials. In the present work are emphasized the results achieved by using a typical assemblage for which the sample was placed on an AISI 1008 steel holder, being that special attention was given for the results obtained for the sample processed at the longer treatment time. The main challenge on the development of the niobium plasma

carburizing process occurred at the heating stage from 300 to 1100°C temperature, since all the carried out treatments presented successive series of arcs (indicated by the red lines falling to zero current values), during their heating stage. The occurrence of arcs was attributed to the discharge geometry aspects as well as the cleanness of the surfaces under plasma species bombardment and the insulating parts. It is worth to be mentioned that for the niobium sample carburized at 200 min, the thermal cycle was interrupted after the last arc (at about 80 min treatment time). After the sample cooling up to the room temperature, the discharge chamber was opened, and the settings of the cathode assemblage and the discharge geometry were successfully revised, making possible to restart the thermal cycle up to complete 200 min, at the carburizing temperature.

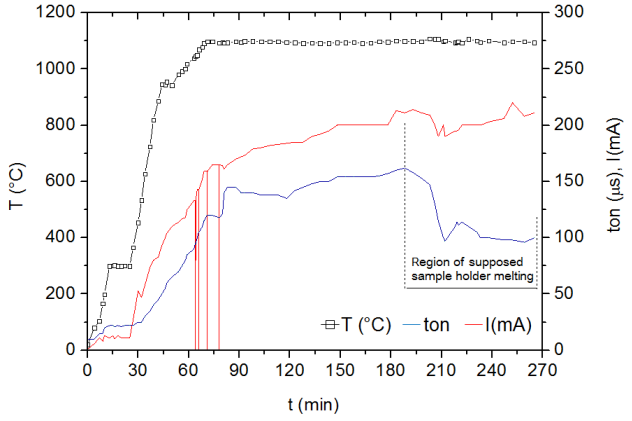

Fig. 2. Evolution of the temperature (*T*), switched-on time of the pulse (*ton*), and current (*I*) as functions of the treatment time for niobium samples carburized at 200 min

Such procedure was adequate enough to provide treatment with no additional arc occurrence. This aspect is to be emphasized, since the change of the discharge regime from the abnormal to the arc one causes interruption of the plasma carburizing treatment. In addition, arcs can cause surface defects on the treated sample surface, and lead the power supply to burn, if high-current protection is not available in the used power system.

Another significant aspect to be considered on the development of the present process deals with the material used to machine the sample support, in this case, AISI 1008 steel. For a long-term treatment (it is the case of the sample carburized at 200 min) under the influence of the carburizing gas mixture, it is suggested that the plasma species bombardment, for the cylindrical geometry of the holder, was able to heat it above the eutectic temperature of the binary system Fe-C (1148°C), and able to enrich its surface for contents above 2.06 wt.% C, which represents the maximum C solubility into the austenite, keeping in mind that the holder material (a typical low-carbon steel) was also subjected to the carburizing treatment, due to the impingent plasma species. Under such conditions, partial melting could occur at the surface of the steel holder. This assumption is confirmed by the results presented in Fig. 3.

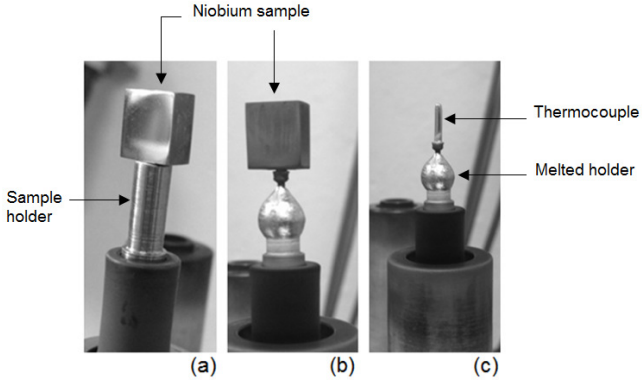

Fig. 3. a) Typical view of the cathode structure assemblage just before performing the carburizing treatment; b), and c) views of the cathode structure just after performing 200 min treatment, and removing the niobium sample from the cathode, respectively

Figure 3a shows a typical view of the cathode structure assemblage just before performing the carburizing treatment. It can be seen, in details, the AISI 1008 steel holder, and the polished niobium sample to be treated. It is also shown in Fig. 3b the cathode structure just after performing the 200 min carburizing treatment, and the new aspect of both the sample holder and the thermocouple after removing the carburized Nb sample (Fig. 3c). The new geometries obtained as for the steel holder as for the thermocouple (noting that the stainless steel coating of the thermocouple was also melted, after exposing it to the plasma species bombardment), after the long-term carburizing treatment, which are typically expected for parts presenting partial melting, clearly prove the above-mentioned assumption. It is also to be noted in Fig. 2 that the evolution of the switched-on time of the pulse (*ton*), which is roughly constant for the range of treatment time 90-190 min, presents a sharp decrease on the *ton* values after 190 min. The authors believe that the partial melting of the steel holder was initiated at the 190 min treatment time. This is based on the fact that in the presence of partial liquid phase, the emission of secondary electrons from the partially melted cathode, and thus the ionization of the plasma next to the niobium sample surrounding were also increased. This aspect would try for to explain why the

necessary *ton* used to keep the carburizing temperature at 1100°C was decreased for a new average value, in the time range indicated between 190-270 min. Aiming to avoid problems associated with melting of the cathode structure, it is clear that another material different from the AISI 1008 steel must be specified to build the sample holder, if the carburizing temperature is equal or higher than 1100°C. The same is valid for the thermocouple material, since the full-scale temperature for the used chromel-alumel thermocouple type-K is on the order of 1280°C, only.

3.2. Characterization of the carburized niobium surfaces

Figure 4 shows typical XRD patterns obtained for the niobium samples carburized at 10, 90, and 200 min. For comparison purpose, it is also shown results obtained for the untreated niobium sample. As the carburizing time is increased, the intensity of the Nb(200) peak tends to decrease, due to a more effective formation of NbC, and $Nb_6C_{4.73}$ at the treated surfaces. The obtainment of carburized layers was confirmed by SEM analysis. SEM characterization was performed at the polished and chemically etched cross-sections of the studied samples. The microstructures were revealed using the etchant ASTM 160 (constituted of 40 ml HS, 30 ml H_2SO_4, 10 ml HNO_3, and 100 ml H_2O). Figures 5a-c shows typical SEM micrographs of the samples carburized at 10, 90, and 200 min, respectively. Carburized layer thickness average (standard deviation) values on the order of 1.20 (0.15), 1.45 (0.10), and 10.50 (0.25) mm were obtained for samples treated at 10, 90, and 200 min. Regarding the kinetics of the carburized layer formation these data were plotted as a function of the carburized time square root ($t^{1/2}$), in Fig. 6, keeping in mind that for the authors of this work it is considered that the plasma carburizing process is thermally activated, or diffusion dependant, and that all treatments were carried out at a same temperature. Here, special attention is to be given to the results related to the sample carburized at 200 min. It is to be noted that at the 200 min carburized sample ($t^{1/2}$ = 1.83), the obtained point in the plot strongly deviates from the linearity projected for the two other studied conditions, namely from the sample carburized at 10, and 90 min ($t^{1/2}$ = 0.41, and 1.22), respectively. Considering that the present plasma assisted carburizing process is diffusion controlled, Fig. 6 results would indicate that the treatment temperature of the sample carburized at 200 min was significantly higher than 1100°C. This assumption is supposedly true, since the stainless steel covering the chromel and alumel wires of the thermocouple used in such experiment was melted, leading the referred wires to be exposed (according to Fig. 3b,c) thus also subjected to plasma species bombardment. This event would possibly lead to erroneous temperature measurements being a possible explanation for the assumption of a supposed higher temperature occurring to the 200 min carburized sample.

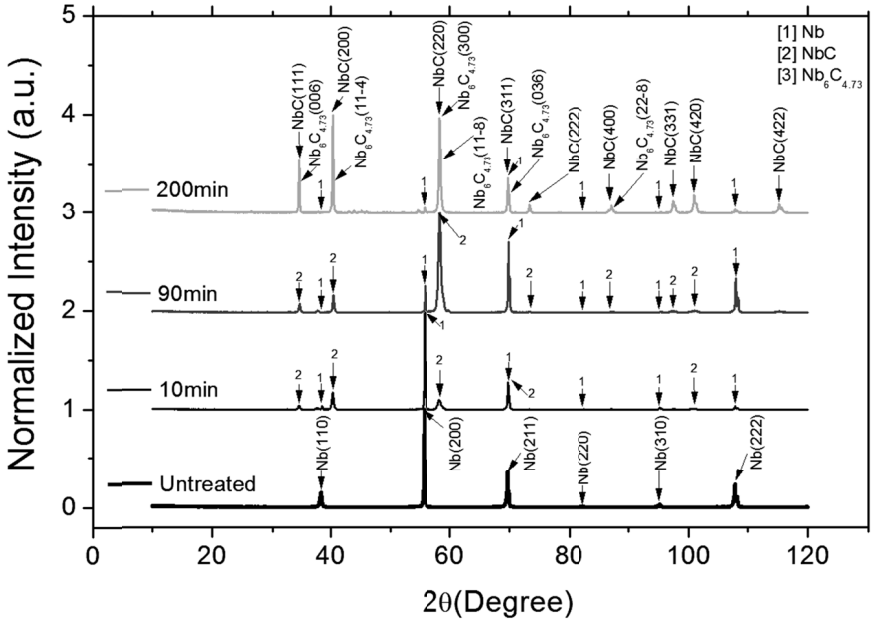

Fig. 4. Typical XRD patterns obtained for untreated niobium samples and carburized at 10, 90, and 200 min

a)

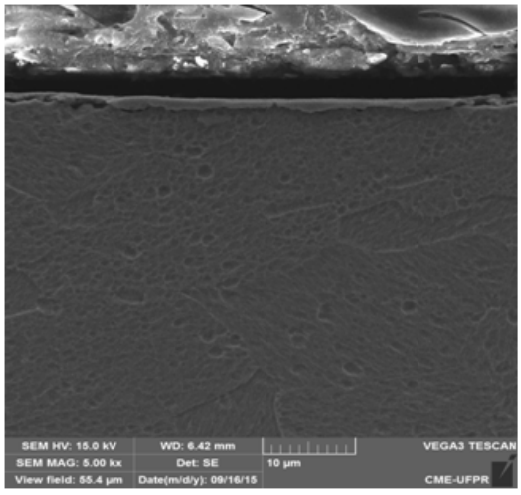

b)

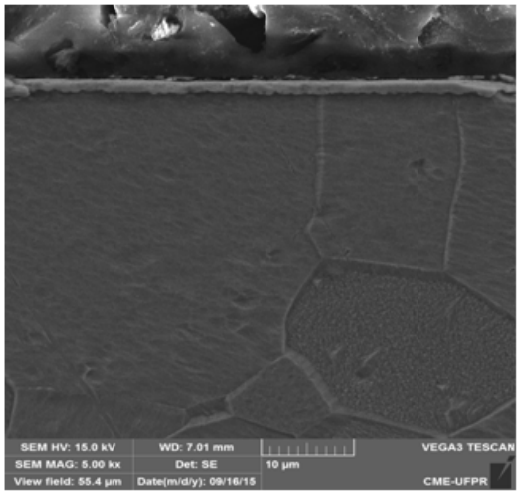

c)

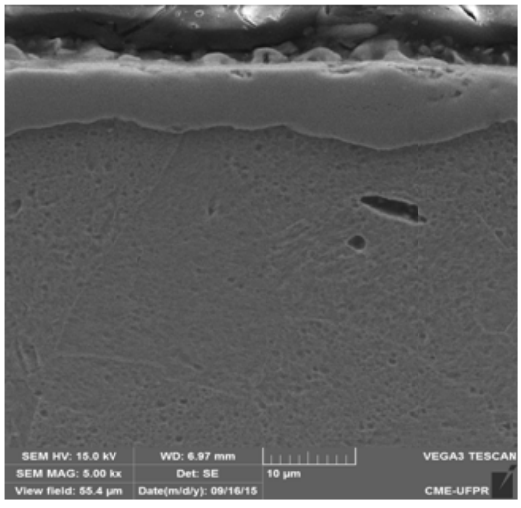

Fig. 5. Typical SEM micrographs of the samples carburized at: a) 10; 90; and 200 min

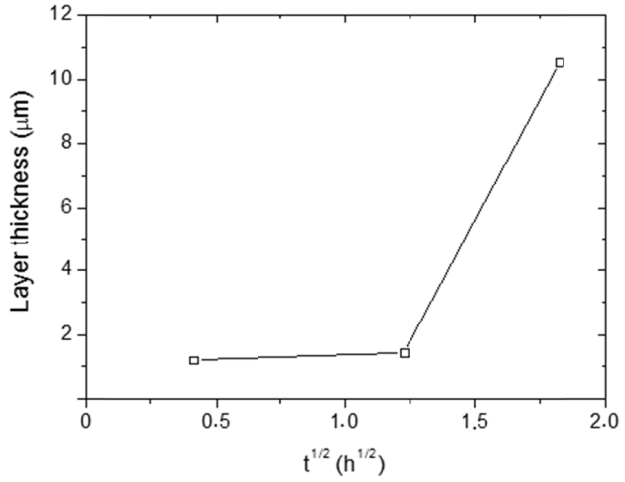

Fig. 6. Carburized layer thickness plotted as a function of the carburized time square root

a)

b)

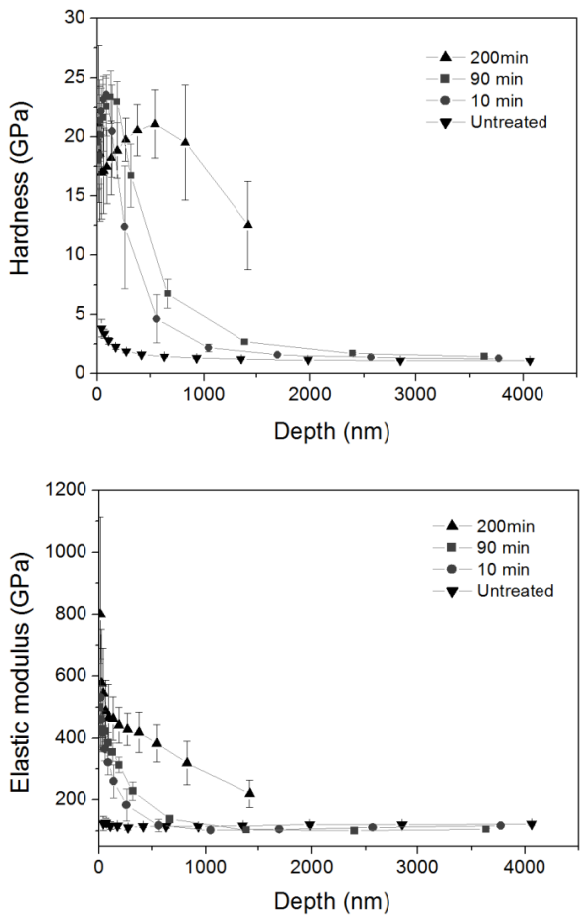

Fig. 7. Nanoindentation test results for: a) hardness; and b) elastic modulus as a function of the indenter contact depth for the studied sample surfaces

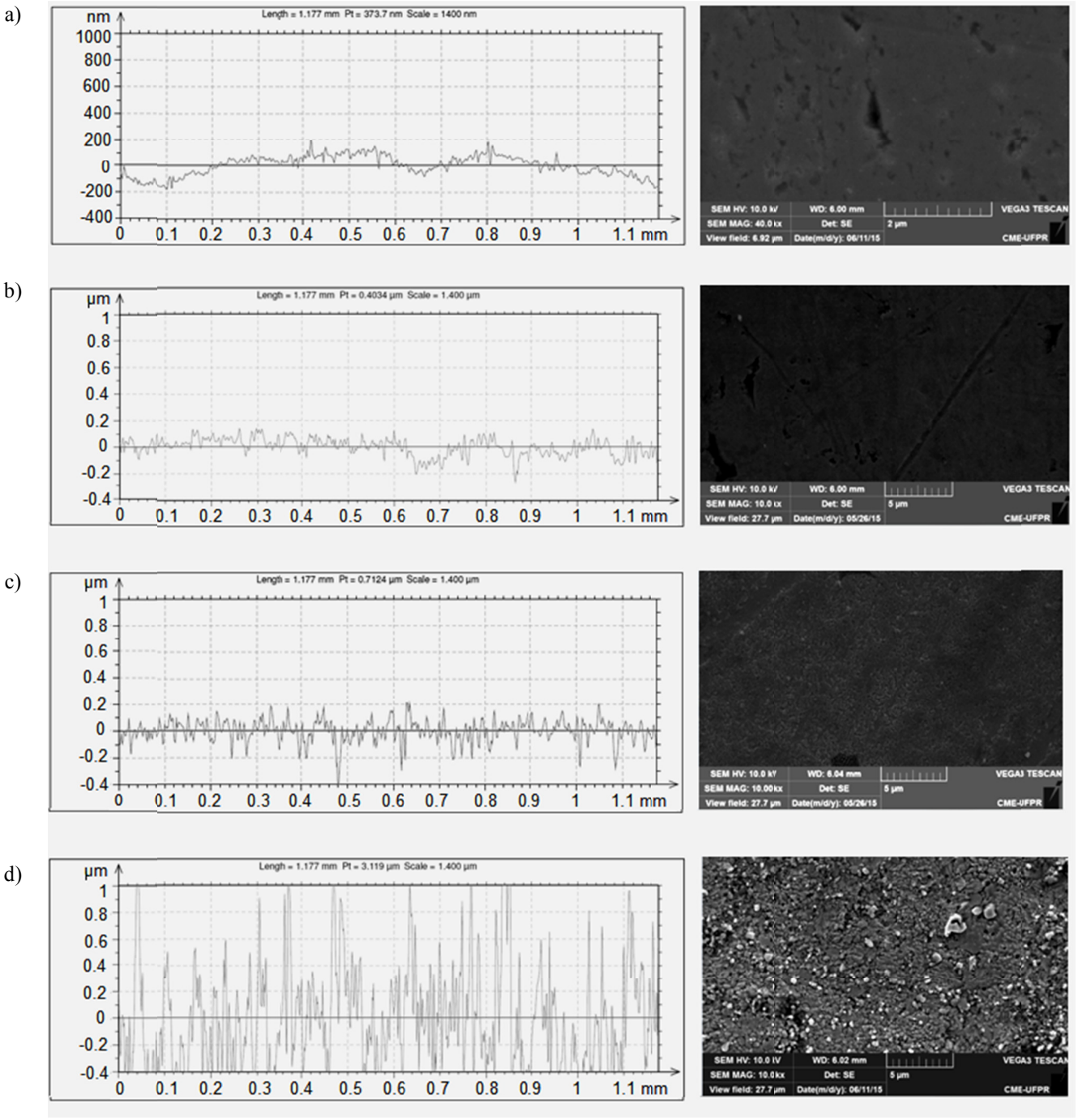

Fig. 8. 2D profiles and SEM images obtained for niobium samples at: a) untreated; and carburized at b) 10; c) 90; and d) 200 min

Figures 7a,b show nanoindentation test results presenting the hardness and elastic modulus curves as a function of the indenter penetration or contact depth for the studied sample surfaces, respectively. The higher hardness values were about 20-25 GPa for all carburized samples. For contact depths up to 500 nm, elastic modulus on average of about 400-500 GPa was obtained. It is to be noted that, for the sample carburized at 200 min, at the shallowest contact depth, average value of 800 GPa presenting an upper limit value on the order of 1100 GPa was verified. This highest

elastic modulus value is at least 10 times higher than that verified for pure niobium (which presents elastic modulus of 103 GPa). The great increment of the elastic modulus verified for the carburized surfaces in comparison with that of the untreated niobium is in agreement with the expected for surfaces presenting NbC phase formation.

Figure 8a-d shows 2D profiles and SEM images obtained for niobium samples at untreated, and carburized at 10, 90, and 200 min, respectively. Results clearly indicate that as the carburizing time is increased, rougher surfaces tend to be formed. This characteristic is typically obtained at the plasma assisted surface processing, since the growth mechanism of niobium carbide phases tends to comprise the formation of small islands of Nb and C atoms clustering, being nucleated at the treated surface, as the surface is enriched with C atoms diffusing into the substrate bulk.

Figures 9a-d show the penetration profile results and the aspect of the scratches obtained by SEM analysis, obtained by making the indenter tip to run along of about 700 μm length for niobium samples at untreated, and carburized at 10, 90, and 200 min, respectively. The penetration residual morphology results obtained for the 200 min carburized sample are worth to be emphasized, since strong recovering clearly indicating an elastic behavior tendency was evidenced in this case, by comparing with that verified for the untreated sample.

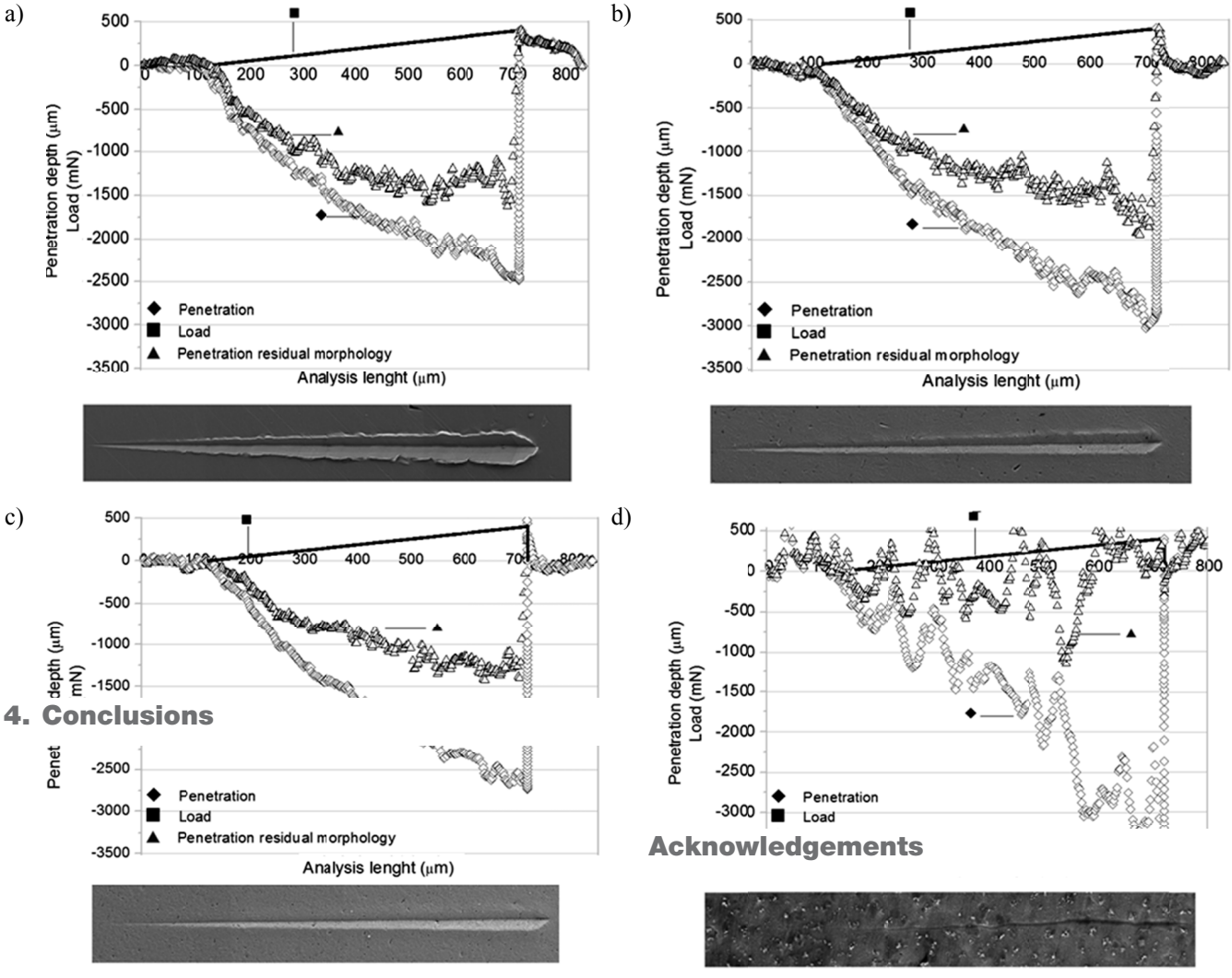

Fig. 9. Penetration profile results and the aspect of the scratches obtained by SEM analysis, for niobium samples at: a) untreated; and carburized at b) 10; c) 90; and d) 200 min

4. Conclusions

Acknowledgements

4. Conclusions

Initial results on the niobium plasma carburizing process development were presented here. Plasma carburizing of niobium samples was successfully carried out, leading to the formation of niobium carbide in niobium substrates. The main challenges related to the risk of arc formation and temperature control during the surface treatment process, allied to aspects of the carburized layer formation kinetics and the phases formed in the niobium treated surfaces were also presented. The niobium carbide phases attained at the treated surfaces can lead to hard surfaces presenting scratches with high elastic recovering degree.

Acknowledgements

This work was supported by CNPq, *Fundação Araucária* of the *Paraná* State, CNPq-Universal Grant N. 482380/2012-8, and MCTI/CNPq/CT-*Aquaviário* Grant N. 456347/2013-5. The authors also wish to express their thanks to the Laboratory of X-ray Optics and Instrumentation (LORXI) and Laboratory of Minerals (LAMIR) from UFPR, by the use of the XRD and SEM equipments.

References

[1] B. Chapman, Glow discharge processes: sputtering and plasma etching, Wiley-Interscience, New York-Chichester-Brisbane-Toronto-Singapore, 1980.

[2] A. Ricard, Reactive plasmas, Société Française du Vide, Plasmas Reactifs, France, 1995, 156.

[3] Y.P. Raizer, Gas Discharge Physics, Corrected 2nd Printing, Springer Verlag, Berlin-Germany, 1997.

[4] J.R. Roth, Industrial Plasma Engineering, The Institute of Physics Volume 1: Principles, Institute of Physics Publishing, Bristol-Philadelphia, 1995.

[5] V.A. Engel, Ionized Gases. Second Edition, American Institute of Physics, New York-USA, 1965.

[6] A.N. Allenstein, R.P. Cardoso, K.D. Machado, S. Weber, K.M.P. Pereira, C.A.L. dos Santos, Z. Panossian, A.J.A. Buschinelli, S.F. Brunatto, Strong evidences of tempered martensite-to-nitrogen-expanded austenite transformation in CA-6NM steel, Materials Science and Engineering A 552 (2012) 569-572.

[7] C.J. Scheuer, R.P. Cardoso, R. Pereira, M. Mafra, S.F. Brunatto, Low temperature plasma carburizing of martensitic stainless steel, Materials Science and Engineering A 539 (2012) 369-372.

[8] C.J. Scheuer, R.P. Cardoso, F.I. Zanetti, T. Amaral, S.F. Brunatto, Low-temperature plasma carburizing of AISI 420 martensitic stainless steel: Influence of gas mixture and gas flow rate, Surface and Coatings Technology 206 (2012) 5085-5090.

[9] C.J. Scheuer, R.P. Cardoso, M. Mafra, S.F. Brunatto, AISI 420 martensitic stainless steel low temperature plasma assisted carburizing kinetics, Surface and Coatings Technology 214 (2013) 30-37.

[10] A.N. Allenstein, C.M. Lepienski, A.J.A. Buschinelli, S.F. Brunatto, Improvement of the cavitation erosion resistance for low-temperature plasma nitrided CA-6NM martensitic stainless steel, Wear 309 (2014) 159-165.

[11] A.N. Allenstein, C.M. Lepienski, A.J.A. Buschinelli, S.F. Brunatto, Plasma nitriding using high H_2 content gas mixtures for a cavitation erosion resistant steel, Applied Surface Science 277 (2013) 15-24.

[12] A.N. Klein, R.P. Cardoso, H.C. Pavanati, C. Binder, A.M. Maliska, G. Hammes, D. Fusão, A. Seeber, S.F. Brunatto, J.L.R. Muzart, DC plasma technology applied to powder metallurgy: an overview, Plasma Science and Technology 15(1) (2013) 70-81.

[13] S.F. Brunatto, J.L.R. Muzart, Influence of the gas mixture flow on the processing parameters of hollow cathode discharge iron sintering, Journal of Physics D: Applied Physics 40 (2007) 3937-3944.

[14] R.S. Mason, R.M. Allott, The Theory of Cathodic Bombardment in a Glow Discharge by Fast Neutrals, Journal of Physics D: Applied Physics 27 (1994) 2372-2378.

[15] I. Abril, A. Gras Marti, Energy Transfer Processes in Glow Discharges, Journal of Vacuum Science & Technology A 4/3 (1986) 1773-1778.

[16] R.S. Mason, M. Pichilingi, Sputtering in a Glow Discharge Ion Source - Pressure Dependence: Theory and Experiment, Journal of Physics D: Applied Physics 27 (1994) 2363-2371.

[17] C. Borcz, C.M. Lepienski, S.F. Brunatto, Surface modification of pure niobium by plasma nitriding. Surface and Coatings Technology 224 (2013) 114-119.

[18] A.V. Linde, V.V. Grachev, R.-M. Marin-Ayral, Self-propagating high-temperature synthesis of cubic niobium nitride under high pressures of nitrogen, Chemical Engineering Journal 155 (2009) 542-547.

[19] R. Musenich, P. Fabbricatore, G. Gemme, R. Parodi, M. Viviani, B. Zhang, V. Buscaglia, C. Bottino, Growth of niobium nitrides by nitrogen-niobium

reaction at high temperature, Journal of alloys and compounds 209 (1994) 319-328.
[20] P.M. Amaral, J.C. Fernandes, L.G. Rosa, D. Martínez, J. Rodríguez, N. Shohoji, X-ray diffraction characterization of carbide and carbonitride if Ti and Zr prepared through reaction between metal powders and carbon powders in a solar furnace, International Journal of Refractory Metals and Hard Materials 17 (2000) 437-443.
[21] W. Wang, Z. Xu, Z. He, Z. Wang, P. Zhang, Study on double-glow plasma niobium surface alloying of pure titanium, Vacuum 81 (2007) 937-942.
[22] Q. Wang, P.Z. Zhang, D.B. Wei, X.H. Chen, R.N. Wang, H. Wang, K. Feng, Microstructure and sliding wear behavior of pure titanium surface modified by double-glow plasma surface alloying with Nb, Materials & Design 52 (2013) 265-273.
[23] U. Sen, S.S. Pazarlıoglu, S. Sen, Niobium boride coating on AISI M2 steel by boro-niobizing treatment, Materials letters 62 (2008) 2444-2446.
[24] G.A. Fontalvo, V. Terziyska, C. Mitterer, High-temperature tribological behaviour of sputtered NbN_x thin films, Surface and Coatings Technology 202 (2007) 1017-1022.
[25] I. Jauberteau, J.L. Jauberteau, M.N. Semeria, Plasma nitriding of thin molybdenum layers at low temperature, Surface and Coatings Technology 116 (1999) 222-228.
[26] I. Jauberteau, J.L. Jauberteau, P. Goudeau, Investigations on a nitriding process of molybdenum thin films exposed to (Ar-N_2-H_2) expanding microwave plasma, Surface and Coatings Technology 203 (2009) 1127-1132.
[27] S.F. Brunatto, A.N. Allenstein, C.L.M. Allenstein, Cavitation erosion behaviour of niobium, Wear 274 (2012) 220-228.
[28] ASM International Handbook Committee, ASM Handbook Volume 2, 10th ed., 1990.
[29] L. Wang, J. Sun, J. Sun, Y. Lv, S. Li, S. Ji, Z. Wen, Niobium nitride modified AISI 304 stainless steel bipolar plate for proton exchange membrane fuel cell, Journal of Power Sources 199 (2012) 195-200.
[30] W.D. Wilkinson, Fabrication of Refractory Metals. No. TID-25424, 1970.
[31] J.J. Olaya, L. Huerta, S.E. Rodil, R. Escamilla, Superconducting niobium nitride films deposited by unbalanced magnetron sputtering, Thin Solid Films 516 (2008) 8768-8773.
[32] Y. Gotoh, M. Nagao, T. Ura, H. Tsuji, J. Ishikawa, Ion beam assisted deposition of niobium nitride thin films for vacuum microelectronics devices, Nuclear Instruments and Methods in Physics Research Section B: Beam Interactions with Materials and Atoms 148 (1999) 925-929.
[33] N. Cansever, Properties of niobium nitride coatings deposited by cathodic arc physical vapor deposition, Thin Solid Films 515 (2007) 3670-3674.
[34] G. Ramírez, S.E. Rodil, H. Arzate, S. Muhl, J.J. Olaya, Niobium based coatings for dental implants, Applied Surface Science 257 (2011) 2555-2559.

Additional information

Selected issues related to this paper are planned to be presented at the 22nd Winter International Scientific Conference on Achievements in Mechanical and Materials Engineering Winter-AMME'2015 in the framework of the Bidisciplinary Occasional Scientific Session BOSS'2015 celebrating the 10th anniversary of the foundation of the Association of Computational Materials Science and Surface Engineering and the World Academy of Materials and Manufacturing Engineering and of the foundation of the Worldwide Journal of Achievements in Materials and Manufacturing Engineering.